Unusual Structural Features of Tetrakis(μ-carboxylato)dirhodium(II), an Antitumor Agent, Bound to Azathioprine, a Biologically Active Mercaptopurine Derivative

H. T. Chifotides,† K. R. Dunbar,*,‡ and J. H. Matonic

Department of Chemistry, Michigan State University, East Lansing, Michigan 48824

N. Katsaros

N.R.C.P.S. "Demokritos", 15310 Ag. Paraskevi Attikis, Greece

Received March 3, 1992

We are investigating the chemistry of azathioprine (6-[1-methyl-4-nitroimidazol-5-yl)thio]purine, AZA), a derivative of the anticancer agent 6-mercaptopurine (6-MP). The considerable biological activity of AZA combined with its electronically and stereochemically versatile binding sites prompted us to investigate the X-ray crystal structure of the bis adduct $[Rh_2(OAc)_4(AZA)_2]\cdot 4DMAA$ (**1**). Crystals of **1** are monoclinic, space group $P2/n$, with unit cell parameters $a = 18.053$ (3) Å, $b = 8.181$ (4) Å, $c = 19.523$ (7) Å, $\alpha = 90°$, $\beta = 97.79$ (5)°, $\gamma = 90°$, $V = 2856$ (3) Å^3, and $Z = 2$. Residuals of $R = 0.064$ and $R_w = 0.082$ and a quality of fit of 2.18 were obtained. The molecule resides on a crystallographic center of inversion at the midpoint of the Rh–Rh bond with AZA coordinated to the two axial positions of the dirhodium tetraacetate cage through the purine nitrogen atom N(3). The metal–metal distance is Rh(1)–Rh(1′) = 2.373 (3) Å and the axial ligand bond length is Rh(1)–N(3) = 2.23 (1) Å. Presumably, steric constraint imposed by the octahedral environment about the rhodium atom together with the bulk of the imidazole ring on S(1) inhibits metal binding at the N(7) site usually observed for purines. The structure is stabilized by hydrogen bonding between N(9)–H and the acetate O(2), detected in solution by the two inequivalent sets of acetates in the variable-temperature ^{1}H NMR spectrum of **1** at −70 °C. Compound **1** has been fully characterized by NMR, IR, and UV–visible spectroscopies as well as by FAB-MS and cyclic voltammetry.

Introduction

There is considerable interest in the chemistry of tetrakis(μ-carboxylato)dirhodium(II) complexes with nucleic acid bases because these complexes function as antitumor agents against many types of tumors.[1,2b,d,e,g] Although the exact mechanism of action is unknown, it is postulated that the biological effect of rhodium(II) carboxylates is due to inhibition of DNA replication and protein synthesis,[2a,b,e,g] with minimal inhibition of RNA synthesis. Indeed, rhodium carboxylates bind axially and reversibly to adenosine[2c,f,h–k,m] and polyadenosine nucleotides,[2b] single-stranded DNA,[2l] and sulfur-containing amino acids and proteins,[2d,g,3d,e] whereas they bind irreversibly to sulfydryl-containing compounds such as cysteine and glutathione, resulting in breakage of the carboxylate cage and liberation of the carboxylate ions.[3a–c] The interaction with the sulfydryl groups has been related to their antitumor activity since enzymes such as DNA polymerase A, essential for DNA synthesis, contain such groups.[2b]

Azathioprine (6-[1-methyl-4-nitroimidazol-5-yl)thio]purine, AZA)[4,24] (II) (Imuran) is a slow release prodrug of the antimetabolite[6c,d] 6-mercaptopurine (6-MP) (I) (Purinethiol),

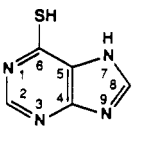

(I) 6-MP

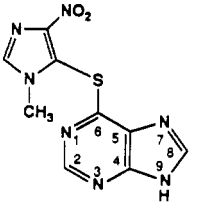

(II) AZA

which is used as an established clinical agent for the treatment of human leukemias.[5,22a] There are several reasons for substituting the sulfydryl group of 6-MP with the protective nitroimidazolyl

† On leave from N.R.C.P.S. "Demokritos".

‡ Camille and Henry Dreyfus Teacher Scholar 1991–1995 and Fellow of the Alfred P. Sloan Foundation 1992–1994.

(1) (a) Hughes, R. G.; Bear, J. L.; Kimball, A. P. *Proc. Am. Assoc. Cancer Res.* **1972**, *13*, 120. (b) Lee, S. H.; Chao, D. L.; Bear, J. L.; Kimball, A. P. *Cancer Chemother. Rep.* **1975**, *59*, 661. (c) Erck, A.; Sherwood, E.; Bear, J. L.; Kimball, A. P. *Cancer Res.* **1976**, *36*, 2204. (d) Howard, R. A.; Sherwood, E.; Erck, A.; Kimball, A. P.; Bear, J. L. *J. Med. Chem.* **1977**, *20*, 943. (e) Kadish, K. M.; Das, K.; Howard, R.; Dennis, A.; Bear, J. L. *Bioelectrochem. Bioener.* **1978**, *5*, 741. (f) Hall, L. M.; Speer, R. J.; Ridgway, H. J. *J. Clin. Hematol. Oncol.* **1980**, *10*, 25.

(2) (a) Erck, A.; Rainen, L.; Whileyman, J.; Chang, I.; Kimball, A. P.; Bear, J. L. *Proc. Soc. Exp. Biol. Med.* **1974**, *145*, 1278. (b) Bear, J. L.; Gray, H. B.; Rainen, L.; Howard, R.; Serio, G.; Kimball, A. P. *Cancer Chemother. Rep., Part I* **1975**, *59*, 611. (c) Rainen, L.; Howard, R. A.; Kimball, A. P.; Bear, J. L. *Inorg. Chem.* **1975**, *14*, 2752. (d) Bear, J. L.; Howard, R. A.; Dennis, A. M. *Curr. Chemother.* **1978**, 1321. (e) Howard, R. A.; Kimball, A. P.; Bear, J. L. *Cancer Res.* **1979**, *39*, 2568. (f) Pneumatikakis, G.; Hadjiliadis, N. *J. Chem. Soc., Dalton Trans.* **1979**, 596 and references therein. (g) Rao, P. N.; Smith, M. L.; Pathak, S.; Howard, R. A.; Bear, J. L. *J. Natl. Cancer Inst.* **1980**, *64*, 905. (h) Farrell, N. *J. Chem. Soc., Chem. Commun.* **1980**, 1014. (i) Farrell, N. *Inorg. Biochem.* **1981**, *14*, 261. (j) Rubin, J. R.; Sundaralingam, M. *J. Biomol. Struct. Dyn.* **1984**, *2*, 525. (k) Alberding, N.; Farrell, N.; Crozier, E. D. *J. Am. Chem. Soc.* **1985**, *107*, 384. (l) Farrell, N.; Vargas, M. D.; Mascarenhas, Y. A.; Gambardella, M. T. P. *Inorg. Chem.* **1987**, *26*, 1426. (m) Rubin, J. R.; Haromy, T. P.; Sundaralingam, M. *Acta Crystallogr.* **1991**, *C47*, 1712.

(3) (a) Howard, R. A.; Spring, T. G.; Bear, J. L. *Cancer Res.* **1976**, *36*, 4402 and references therein. (b) Bear, J. L.; Howard, R. A.; Dennis, A. M. *Curr. Chemother.* **1978**, 1321. (c) Pneumatikakis, G.; Psaroulis, P. *Inorg. Chim. Acta* **1980**, *46*, 97. (d) Dennis, A. M.; Howard, R. A.; Bear, J. L. *Inorg. Chim. Acta* **1982**, *66*, L31. (e) Chen, J.; Kostic, N. M. *Inorg. Chem.* **1988**, *27*, 2682.

(4) Yeowell, H. N.; Elion, G. B. *J. Heterocycl. Chem.* **1973**, *10*, 1017.

(5) (a) Miner, R. W. *Ann. N.Y. Acad. Sci.* **1954**, *60*, 183. (b) Van Scoik, K. G.; Johnson, C. A.; Porter, W. R. *Drug Metabolism Rev.* **1985**, *16* (1&2), 157 and references therein.

(6) (a) Elion, G. B.; Callahan, S.; Rundles, R. W.; Hitchings, G. H. *Cancer Res.* **1963**, *23*, 1207. (b) Elion, G. B.; Hitchings, G. H. In *Handbook of Experimental Pharmacology*; Eichler, O., Farah, A., Herken, H., Welch, A. D., Eds.; Springer-Verlag: New York, 1975; Vol. 38, p 404. (c) Langen, P. In *Antimetabolites of Nucleic Acid Metabolism*; Gordon & Breach: New York, 1975; p 162. (d) Pullman, B.; Pullman, A. In *Quantum Biochemistry*; Interscience: New York, 1963; p 240.

0020-1669/92/1331-4628$03.00/0

group; these are to protect the –SH group of 6-MP from in vivo methylation, to alter the metabolism and distribution of the drug, and to improve the targeting of 6-MP toward tumor cells by preferentially liberating the thiopurine in the tumor[5b] since it is known that reaction of AZA with sulfydryl groups of proteins slowly converts AZA to 6-MP or to thioguanine.[6a,b] After cleavage of the nitroimidazolyl group from the sulfur atom, AZA is metabolically identical to 6-MP. The cytostatic activity of these antimetabolites is attributed to (a) feedback inhibition of the first enzyme in de novo ribonucleotide synthesis, (b) inhibition of purine ribonucleotide interconversion, and (c) indirect incorporation into DNA after intracellular conversion to 6-thioguanine.[5b,6a,b] Apart from the antitumor activity of AZA, which in some cases proved to have a superior chemotherapeutic index than 6-MP,[6a,b] AZA is widely used as an immunosuppressant in preventing the rejection of various transplanted organs including kidney, liver, and bone marrow[5,6c,7] as well as an antiinflammatory agent in the treatment of autoimmune diseases such as rheumatoid arthritis and systemic lupus erythematosus.[5b,7]

Besides the biochemical implications, the coordination chemistry of AZA with metals is of interest due to the electronically and stereochemically versatile binding sites of the drug. Indeed, as a purine it offers multiple binding sites[10] including N(1), N(3), N(7) and N(9), while the presence of sulfur (available for "soft" metals) introduces new chemical, structural, and spectroscopic features to the molecule by rendering it similar to other reactive biomolecules such as methionine, biotin, penicillin, etc., which are all thioethers.[11] Crystal structures of biologically active ligands with metals are important for the understanding of factors affecting metal transport, issues that are related to the design of new metal-mediated repository, slow-release, or long-acting drugs. It has been found that certain metal complexes of 6-mercaptopurine show antitumor activity which is enhanced with respect to the activity of the free ligand.[8] In spite of this, only six crystal structures of 6-MP with metals, namely Cu(II), Cu(I), Ru(II), Cd(II), and Hg(II), have been reported to date.[9] In these, 6-MP acts either as a monodentate bridging or nonbridging ligand through its S(6) atom or as a S(6)/N(7) chelating ligand.[9] To our knowledge, no corresponding X-ray studies of AZA–metal complexes have been reported until the present work. Herein we report the structural characterization of the bis adduct of tetrakis(μ-carboxylato)dirhodium(II) with azathioprine in the solid state and in solution.

Experimental Section

Starting Materials. $Rh_2(OAc)_4(H_2O)_2$ was purchased from Merck Chemicals and was used without further purification. Azathioprine (AZA) was purchased from Sigma and donated by the Wellcome Co.; in both instances, it was used without further purification. N,N-Dimethylacetamide (DMAA) (Spectrograde) was purchased from Aldrich Chemical Co. and was used as received. All preparative manipulations were carried out at room temperature in an open atmosphere.

Preparation and Crystallization of $[Rh_2(OAc)_4(AZA)_2]$·4DMAA (1). A clear yellow solution of AZA (0.115 g, 0.41 mmol) in ca. 3 mL of DMAA was added to a bright green solution of $Rh_2(OAc)_4(H_2O)_2$ (0.100 g, 0.21 mmol) in ca. 7 mL of DMAA at room temperature. After the two solutions were mixed, an immediate color change from green to red ensued, after which time the reaction was stirred for ca. 1 h to allow for complete reaction. A crop of red needlelike crystals was obtained after slow evaporation of the solvent in air for several days; yield 0.234 g (83%). It is important that the reaction volume not exceed ca. 10 mL for this scale of preparation, as it appears that the product reverts to the free starting material under dilute conditions in DMAA. Anal. Calcd for $C_{38}H_{53}N_{17}O_{15}S_2Rh_2$ (3 DMAA per molecule of **1**): C, 36.28; H, 4.25; N, 18.92. Calcd for $C_{42}H_{62}N_{18}O_{16}S_2Rh_2$, (4 DMAA per molecule of **1**): C, 37.50; H, 4.65; N, 18.74). Found: C, 36.13; H, 4.75; N, 17.50. Although the crystallographic and the NMR data support four DMAA molecules per dirhodium unit, the elemental analysis is not in complete accord due to loss of solvent. Fast atom bombardment mass spectrometry (FAB-MS): highest mass peak is m/z = 997.1 for $Rh_2(O_2CCH_3)_4(C_9H_7N_7O_2S)_2$. IR spectral data (KBr, pellet, range 4000–200 cm^{-1}), cm^{-1}: ν(N–H) = 3404 m, 3348 m, $\nu(C–H_{arom})$ = 3100 s, $\nu(C–H_{arom})$ = 3068 w, ν(N9–H) = 2932 s, 1731 m (overtone), ν(C=O, DMAA) = 1636 s, $\nu_{as}(COO^-)$ = 1592 s, {ν(C=C) + ν(C=N) + δ(N9–H)} = 1580 s, $\nu_{as}(NO_2)$ = 1538 s, 1494 s, $\nu_{sym}(COO^-)$ = 1432 s, $\delta_{as}(CH_3)$ = 1401 s, $\nu_{sym}(NO_2)$ = 1375 m, $\delta_{sym}(CH_3)$ = 1330 m, 1298 m, [δ(N–C–N) + ν(C–N) + γ(N9–H)] = 1240 s, 1136 w; ring breathing vibrations + C–H in-plane deformations = 1008 m, 998 s; out-of-plane C–H deformations for purine = 926 m, 866 s; out of plane C–H deformations for imidazole = 833 vs, 627 m, 615 m, 494 w, $\nu_{as}(Rh–O_{eq})$ = 381, $\nu_{sym}(Rh–O_{eq})$ = 334 (ν = stretching mode, δ = bending mode). Electronic spectrum (quartz, CH_2Cl_2, range 200–800 nm), λ_{max}, nm (ϵ_M, M^{-1} cm^{-1}): 532 (368), 442 sh, 342 sh, 279 (2.4×10^4).

Physical Measurements. Infrared spectra were recorded on a Nicolet 740 FT-IR spectrophotometer. ^1H NMR spectra were measured on a Varian 300-MHz or 500-MHz spectrometer. Chemical shifts were referenced relative to the residual proton impurity of CD_2Cl_2-d_2 (5.32 ppm with respect to TMS). Electronic absorption spectra were measured on a Hitachi U-2000 spectrophotometer. Electrochemical measurements were carried out by using an EG&G Princeton Applied Research Model 362 scanning potentiostat in conjunction with a BAS Model RXY recorder. Cyclic voltammetry experiments were carried out at 22 ± 2 °C in CH_2Cl_2 containing 0.1 M tetra-*n*-butylammonium tetrafluoroborate ((TBA)BF_4) as the supporting electrolyte. $E_{1/2}$ values, determined as $(E_{p,a} + E_{p,c})/2$, were referenced to the Ag/AgCl electrode and are uncorrected for junction potentials. The Cp_2Fe/Cp_2Fe^+ couple occurs at $E_{1/2}$ = +0.52 V under the same experimental conditions. Fast atom bombardment (FAB) mass spectrometry studies were performed on a JEOL HX 110 double-focusing mass spectrometer housed in the National Institute of Health/Michigan State University Mass Spectrometry Facility; the sample was dissolved in a 3-nitrobenzyl alcohol matrix. Elemental analyses were performed at Galbraith Laboratories, Inc.

X-ray Crystallographic Procedures. The structure of $[Rh_2(OAc)_4(AZA)_2]$·4DMAA (**1**) was determined by application of general procedures fully described elsewhere.[12] Before complete evaporation of the solvent had occurred, a dark red crystal of **1** with approximate dimensions 0.50 × 0.15 × 0.10 mm^3 was selected and mounted on the tip of a glass fiber with epoxy cement. The crystal was placed on the goniometer in a stream of liquid nitrogen at T = 183 K to avoid rapid loss of the solvent from the crystal lattice at room temperature. Geometric and intensity data were collected on a Nicolet P3/F updated to a Siemens P3/V diffractometer equipped with graphite-monochromated Mo Kα ($\lambda_{\bar{\alpha}}$ = 0.710 73 Å). A rotation photograph was used to locate 14 reflections from which a preliminary cell was indexed. The crystal system was found to be monoclinic; this was verified by axial photography. An accurate cell for data collection was calculated from 25 reflections in the range 15° ≤ 2θ ≤ 25°. One-fourth of the full sphere of data was measured in the range 0,0,–1 to +h,+k,+l by an ω–2θ scan motion in the range 4° ≤ 2θ ≤ 45°. During data collection, three standard reflections were measured every 150 reflections; negligible loss of intensity was observed and thus a correction was not applied. After equivalent reflections were averaged, 4319 unique data remained of which 2316 were observed with $F_o^2 \geq 3\sigma(F_o^2)$. Calculations for **1** were performed on a VAXSTATION 2000 computer by using the Texsan crystallographic software package of Molecular Structure Corp.[13] The space group was determined to be

(7) (a) Mitra, A. K.; Narurkar, M. M. *Int. J. Pharm.* **1986**, *35*, 165. (b) Chan, G. L. C.; Canafax, D. M.; Johnson, C. A. *Pharmacotherapy* **1987**, *7* (5), 165 and references therein.
(8) (a) Kirschner, S.; Wei, Y. K.; Francis, D.; Bergman, J. G. *J. Med. Chem.* **1966**, *9*, 369. (b) Das, M.; Livingstone, S. E. *Br. J. Cancer* **1978**, *38*, 325. (c) Skinner, S. M.; Swatzell, J. M.; Lewis, R. W. *Res. Commun. Chem. Pathol. Pharm.* **1978**, *19*, 165.
(9) Dubler, E.; Gyr, E. *Inorg. Chem.* **1988**, *27*, 1466 and references therein.
(10) (a) Marzilli, L. G.; Kistenmacher, T. J.; Eichhorn, G. L. In *Metal Ions in Biology 1*; Spiro, T. G., Ed.; Wiley: New York, 1980; p 179 and references therein. (b) Barton, J. K.; Lippard, S. J. In *Metal Ions in Biology 1*; Spiro, T. G., Ed.; Wiley: New York, 1980; p 31 and references therein. (c) Lönnberg, H. In *Biocoordination Chemistry*; Burger, K., Ed.; Ellis Horwood Series: London, 1990; p 284.
(11) (a) Mc Cormick, D. B.; Greisser, R.; Sigel, H. In *Metal Ions in Biological Systems*; Sigel, H., Ed.; Dekker: New York, 1974; Vol. 1, p 213. (b) Decock-Le Reverend, B.; Kozlowski, H. *J. Chim. Phys.* **1985**, *82*, 883.
(12) (a) Cotton, F. A.; Frenz, B. A.; Deganello, G.; Shaver, A. *J. Organomet. Chem.* **1973**, 227. (b) Bino, A.; Cotton, F. A.; Fanwick, P. E. *Inorg. Chem.* **1979**, *18*, 3558.
(13) TEXSAN-TEXRAY Structure Analysis Package, Molecular Structure Corp., 1985.

Table I. Crystal Data for $[Rh_2(OAc)_4(AZA)_2]\cdot 4DMAA$ (**1**)

formula	$Rh_2C_{42}N_{18}O_{16}S_2H_{62}$	d_{calc}, g/cm^3	1.532
		cryst size, mm^3	0.50 × 0.15 × 0.10
fw	1344.99	μ (Mo Kα), cm^{-1}	7.1332
space group	$P2/n$	radiation	Mo Kα (λ_α =
a, Å	18.053 (3)	(monochromated	0.710 73 Å);
b, Å	8.181 (4)	in incident beam)	graphite
c, Å	19.523 (7)		monochromated
α, deg	90	temperature, °C	−90 ± 2
β, deg	97.79 (5)	transm factors:	1.09; 0.896
γ, deg	90	max; min	
V, Å^3	2856 (3)	R^a	0.064
Z	2	$R_w{}^b$	0.082

^{a} $R = \sum||F_o| - |F_c||/\sum|F_o|$. ^{b} $R_w = [\sum w(|F_o| - |F_c|)^2/\sum w|F_o|^2]^{1/2}$; $w = 1/\sigma^2(|F_o|)$.

Table II. Atomic Positional Parameters and Equivalent Isotropic Displacement Parameters and their Estimated Standard Deviations for $[Rh_2(OAc)_4(AZA)_2]\cdot 4DMAA$ (**1**)

atom	x	y	z	B_{eq},^{a} Å^2
Rh(1)	0.93391 (6)	0.0124 (1)	0.49149 (5)	1.79 (4)
S(1)	0.5728 (2)	0.2355 (4)	0.4461 (2)	2.3 (2)
O(1)	0.9269 (5)	−0.215 (1)	0.5299 (5)	2.4 (4)
O(2)	0.9349 (5)	−0.078 (1)	0.3948 (4)	2.3 (4)
O(3)	0.9418 (5)	0.100 (1)	0.5884 (4)	2.2 (4)
O(4)	0.9487 (5)	0.240 (1)	0.4551 (4)	2.3 (4)
O(5)	0.6364 (7)	0.584 (1)	0.4292 (7)	4.9 (6)
O(6)	0.638 (1)	0.768 (2)	0.5054 (6)	7.5 (9)
O(7)	0.1658 (5)	0.351 (1)	0.6929 (5)	3.1 (5)
O(8)*	−0.1075 (8)	0.499 (2)	0.7278 (7)	6.8 (3)
N(1)	0.7128 (6)	0.212 (1)	0.5122 (5)	2.2 (5)
N(10)	0.5520 (6)	0.312 (1)	0.5775 (6)	2.5 (5)
N(3)	0.8100 (6)	0.048 (1)	0.4755 (6)	1.8 (5)
N(12)	0.5842 (6)	0.568 (1)	0.5949 (6)	2.6 (6)
N(13)	0.6245 (7)	0.631 (2)	0.4847 (8)	3.6 (7)
N(7)	0.6484 (6)	−0.024 (1)	0.3539 (5)	2.4 (5)
N(9)	0.7677 (6)	−0.111 (1)	0.3730 (6)	2.0 (5)
N(14)*	−0.169 (1)	0.702 (3)	0.686 (1)	10.3 (6)
N(15)	0.1445 (6)	0.611 (1)	0.7171 (6)	2.8 (6)
C(2)	0.7820 (7)	0.150 (2)	0.5185 (7)	2.2 (6)
C(11)	0.5586 (8)	0.440 (2)	0.6225 (9)	3.4 (8)
C(4)	0.7602 (6)	−0.002 (2)	0.4245 (6)	1.6 (5)
C(13)	0.5957 (7)	0.520 (2)	0.5309 (7)	2.2 (6)
C(5)	0.6865 (7)	0.050 (1)	0.4115 (7)	1.7 (6)
C(14)	0.5769 (7)	0.362 (2)	0.5171 (7)	1.8 (6)
C(6)	0.6640 (7)	0.160 (2)	0.4602 (7)	2.0 (6)
C(15)	0.527 (1)	0.144 (2)	0.594 (1)	5 (1)
C(8)	0.7000 (7)	−0.118 (2)	0.3341 (7)	2.1 (6)
C(16)	0.987 (1)	−0.289 (2)	0.5491 (7)	2.6 (7)
C(17)	0.979 (1)	−0.459 (2)	0.5816 (7)	3.6 (7)
C(18)	0.9967 (8)	−0.113 (1)	0.3745 (7)	2.0 (6)
C(19)	0.9953 (8)	−0.175 (2)	0.3022 (7)	2.6 (6)
C(20)	0.2052 (9)	0.551 (2)	0.6158 (8)	3.9 (8)
C(21)	0.1691 (6)	0.498 (2)	0.6770 (7)	2.9 (6)
C(22)	0.108 (1)	0.565 (2)	0.7769 (8)	4.4 (8)
C(23)	0.147 (1)	0.784 (2)	0.6977 (9)	6 (1)
C(25)*	−0.166 (2)	0.564 (5)	0.690 (2)	14 (1)
C(24)*	−0.104 (1)	0.806 (3)	0.736 (1)	8.8 (7)
C(26)*	−0.228 (2)	0.474 (4)	0.645 (2)	11.0 (8)
C(27)*	−0.225 (2)	0.816 (4)	0.642 (2)	10.7 (8)

^{a} Starred values denote atoms that were refined isotropically. Values for anisotropically refined atoms are given in the form of equivalent isotropic displacement parameter defined as $^4/_3[a^2\beta_{11} + b^2\beta_{22} + c^2\beta_{33} + ab(\cos\gamma)\beta_{12} + ac(\cos\beta)\beta_{13} + bc(\cos\alpha)\beta_{23}]$.

a non-standard setting of space group No. 13 ($P2/n$). The position of the unique Rh atom, which is situated about the inversion center ($0,0,^1/_2$), was located by the direct methods program in SHELXS-86. The positions of the remaining non-hydrogen atoms were located through a sequence of successive difference Fourier maps and least-square cycles. Except for one solvent molecule, all of the non-hydrogen atoms were refined anisotropically. An absorption correction based upon the program DIFABS was applied to the data.[14] A summary of crystallographic parameters is found in Table I. A listing of selected bond distances and angles is given in Table III.

(14) Walker, N.; Stuart, D. *Acta Crystallogr.* **1983**, *A39*, 158.

Table III. Selected Bond Distances (Å) and Bond Angles (deg) for $[Rh_2(OAc)_4(AZA)_2]\cdot 4DMAA$ (**1**)

Bond Distances

Rh(1)–Rh(1′)	2.373 (3)	N(3)–C(2)	1.33 (2)
Rh(1)–O(1)	2.019 (9)	N(3)–C(4)	1.31 (1)
Rh(1)–O(2)	2.029 (9)	N(1)–C(6)	1.32 (2)
Rh(1)–O(3)	2.009 (9)	N(7)–C(5)	1.38 (2)
Rh(1)–O(4)	2.022 (9)	N(7)–C(8)	1.31 (2)
Rh(1)–N(3)	2.23 (1)	N(9)–C(4)	1.36 (2)
O(1)–C(16)	1.26 (2)	N(9)–C(8)	1.35 (2)
O(2)–C(18)	1.27 (2)	C(4)–C(5)	1.39 (2)
O(3′)–C(18)	1.25 (1)	C(5)–C(6)	1.41 (2)
O(4′)–C(16)	1.24 (2)	S(1)–C(14)	1.72 (1)
N(1)–C(2)	1.34 (2)	S(1)–C(6)	1.74 (1)

Hydrogen Bond Distances

N(9)–H(9)···O(2)	3.00 (1)	C(2)–H(2)···O(3)	3.05 (2)

Bond Angles

Rh(1)–Rh(1′)–O(1′)	88.9 (3)	O(2)–Rh(1)–O(4)	89.5 (4)
Rh(1)–Rh(1′)–O(2′)	87.9 (3)	O(2)–Rh(1)–N(3)	93.0 (4)
Rh(1)–Rh(1′)–O(3′)	87.5 (3)	O(2)–C(18)–O(3)	124 (1)
Rh(1)–Rh(1′)–O(4′)	87.1 (3)	O(3)–Rh(1)–O(4)	90.4 (4)
Rh(1)–Rh(1′)–N(3′)	177.4 (3)	O(3)–Rh(1)–N(3)	91.5 (4)
Rh(1)–O(1)–C(16)	117.3 (9)	O(4)–Rh(1)–N(3)	90.5 (4)
Rh(1)–O(2)–C(18)	119.5 (8)	N(1)–C(6)–C(5)	120 (1)
Rh(1)–O(3)–C(18′)	121.5 (9)	N(1)–C(2)–N(3)	128 (1)
Rh(1)–O(4)–C(16′)	119.5 (9)	N(3)–C(4)–N(9)	130 (1)
Rh(1)–N(3)–C(2)	116.9 (9)	N(3)–C(4)–C(5)	126 (1)
Rh(1)–N(3)–C(4)	129.4 (8)	N(7)–C(8)–N(9)	116 (1)
S(1)–C(14)–N(10)	122 (1)	N(7)–C(5)–C(4)	112 (1)
C(5)–N(7)–C(8)	102 (1)	N(7)–C(5)–C(6)	133 (1)
O(1)–Rh(1)–O(2)	91.0 (4)	N(9)–C(4)–C(5)	105 (1)
O(1)–Rh(1)–O(3)	88.8 (4)	C(14)–S(1)–C(6)	98.6 (6)
O(1)–Rh(1)–O(4)	176.0 (4)	C(2)–N(1)–C(6)	118 (1)
O(1)–Rh(1)–N(3)	93.5 (4)	C(2)–N(3)–C(4)	113 (1)
O(1)–C(16)–O(4′)	127 (1)	C(4)–C(5)–C(6)	116 (1)
O(1)–C(16)–C(17)	116 (1)	C(4)–N(9)–C(8)	106 (1)
O(2)–Rh(1)–O(3)	175.5 (4)		

Results and Discussion

X-ray Structure of $[Rh_2(OAc)_4(AZA)_2]\cdot 4DMAA$ (1). As shown in Figure 1, the dirhodium unit is situated on a crystallographic inversion center relating the halves of the molecule. AZA is axially coordinated to the dirhodium tetraacetate cage through the pyrimidine nitrogen N(3), with further stabilization afforded by hydrogen bonds between the N(9)–H atom of the imidazole ring and the acetate O(2), as evidenced by the N(9)–O(2) distance of 3.00 Å (see Table III). This gives rise to two inequivalent sets of acetates in the solid-state and low-temperature solution form (vide infra). The distances Rh(1)–Rh(1′) = 2.373 (3) Å and Rh(1)–N(3) = 2.23 (1) Å (Table III) are within the expected range for aromatic nitrogen donors[15] (for example the pyridine adduct exhibits Rh(1)–Rh(2) = 2.3994 (5) Å and Rh(1)–N(1) = 2.234 (3) Å).[16] Crystallographic data indicate that the AZA ligand is protonated at N(9) unlike in typical cases involving 6-MP wherein the hydrogen is displaced from N(9) to N(7) upon complexation.[17] The N(9)–H presence as opposed to N(7)–H is supported by the interatomic distances and bond angles of the imidazole ring (Table III). The angles C(5)–N(7)–C(8) and C(4)–N(9)–C(8), with respective values of 102 (1) and 106 (1)°, lend further credence to the idea that the AZA ligand is stabilized in the N(9)–H tautomer as found in the free ligand.[18] The values

(15) (a) Felthouse, T. R. In *Prog. Inorg. Chem.*; Lippard, S. J., Ed.; Wiley: New York, 1982; Vol. 29, p 73 and references therein. (b) Boyar, E. B.; Robinson, S. D. In *Coordination Chemistry Reviews*; Lever, A. B. P., Ed.; Elsevier: Amsterdam, 1983; Vol. 50, p 109.
(16) Koh, Y. B.; Christoph, G. G. *Inorg. Chem.* **1978**, *17*, 2590.
(17) Lavertue, P.; Hubert, J.; Beauchamp, A. L. *Inorg. Chem.* **1976**, *15*, 322.
(18) (a) Cook, W. J.; Bugg, C. E. *J. Pharm. Sci.* **1975**, *64* (2), 221. (b) Acharya, K. R. *Proc. Indian Acad. Sci., Chem. Sci.* **1984**, *93* (2), 183.

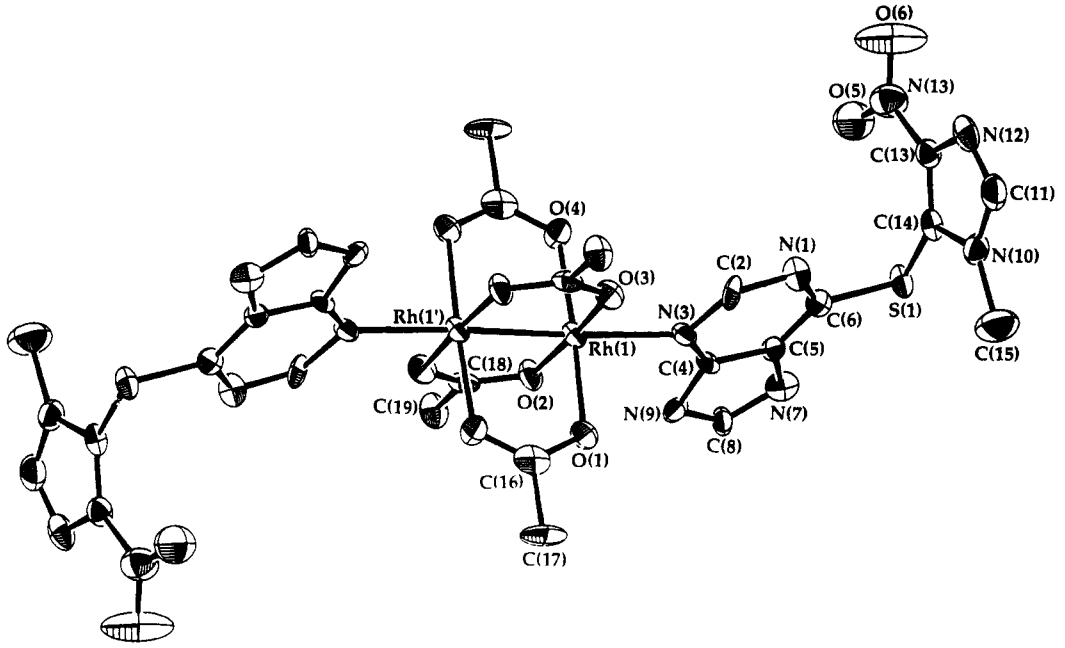

Figure 1. ORTEP representation of $[Rh_2(OAc)_4(AZA)_2]\cdot 4DMAA$ (**1**) with 50% probability ellipsoids.

for the interatomic distances and bond angles of the imidazole ring are in complete accord with those expected for a N(9)–H-substituted purine.[9,17] The N(9)···O(2) distance of 3.00 (1) Å is close in value to the N(9)···N(3) = 2.90 Å hydrogen bond distance formed within a pair of two AZA molecules in the free ligand.[18] The angle N(3)–C(4)–N(9) = 130 (1)° in **1** does not deviate from that in the free ligand,[18] thereby ruling out ligand strain upon complex formation. The C(2)–O(3) distance of 3.05 (2) Å implies an interaction that may be described as a weak hydrogen bond (the H(2) coalesces at −20 °C; vide infra). Ordinarily, carbon is too electropositive to donate a proton to a hydrogen bond, but such donation can occur when the carbon atom is activated by adjacent nitrogens,[19] in this case N(1) and N(3).

The unequal distances N(9)–O(1) = 4.00 Å and N(9)–O(2) = 3.00 Å indicate that the purine plane does not bisect the dihedral angle formed between the two equatorial acetates. Actually, the purine ring forms dihedral angles of 20.80 and 106.00° with the C(18)–O(2)–Rh(1)–O(3) and C(16)–O(1)–Rh(1)–O(4) planes respectively. The dihedral angle between the purine plane and the imidazole plane is 96.25° and the angle C(14)–S(1)–C(6) is 98.6 (6)°, thus the trans relationship of bonds S(1)–C(14) and C(6)–C(5) as is found in the free ligand.[18] The S(1)–C(6) and S(1)–C(14) distances of 1.74 (1) and 1.72 (1) Å, respectively, are nearly identical to those in free AZA, the S(1)–C(14) distance being slightly shorter due to inductive effects of the substituents. A 180° rotation of the imidazole ring around the S(1)–C(14) bond brings the nitro group to the side of N(1) in the purine ring, as opposed to the N(10)–CH_3(15) group as in the free ligand.[18] The mean deviation from planarity of the atoms in the purine ring is 0.015 Å and for the imidazole ring 0.0046 Å, indicating only small distortions. An interesting feature of the three-dimensional packing diagram of compound **1** is that it involves infinite stacking of staggered, partially overlapping, 1-methyl-4-nitroimidazol rings at a distance of ca. 3.3 Å (see packing diagram, Figure 2). Such stacking has been seen in other crystal structures of various purines.[9,17,19]

NMR Spectroscopy. At room temperature, in CD_2Cl_2-d_2, the ^{1}H NMR spectrum of AZA reveals three resonances in the aromatic region at δ +8.61, +8.13 and +7.72 ppm with a 1:1:1 ratio, corresponding to the three aromatic protons H(2), H(8), and H(11) of azathioprine, respectively, and one resonance at δ +3.71 ppm corresponding to CH_3(15) of the nitroimidazole ring (see Table IV). The proton H(11) of the 1-methyl-4-nitroimidazole ring resonates at ca. δ +7.5 ppm,[20a] upfield from the purine protons presumably because, in a purine, the pyrimidine ring is a π-electron deficient system while the imidazole ring is a π-electron rich system.[20b,c] The assignment of the purine protons H(2) and H(8) is based on the ^{1}H NMR spectrum of 8-deute-

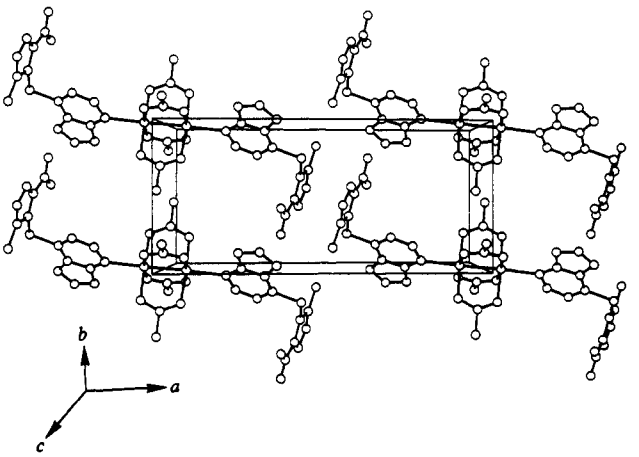

Figure 2. Packing diagram of $[Rh_2(OAc)_4(AZA)_2]\cdot 4DMAA$ (**1**) viewed down the *c* axis. Solvent molecules of crystallization (DMAA) have been omitted for clarity.

Table IV. ^{1}H NMR Data for AZA and $[Rh_2(OAc)_4(AZA)_2]\cdot 4DMAA$ (**1**) in CD_2Cl_2-d_2[a]

compd	solvent	chem shift				
		H(2)	H(8)	H(11)	CH_3(15)	N(9)–H
AZA	CD_2Cl_2-d_2	8.61	8.13	7.72	3.71	*b*
AZA-d_8	CD_2Cl_2-d_2	8.61		7.72	3.71	
1	CD_2Cl_2-d_2	9.28	8.35	7.82	3.85	11.65

[a] All chemical shift values are reported in ppm for spectra recorded at room temperature. [b] The N(9)–H resonance for AZA in CD_2Cl_2-d_2 is not observed due to its low solubility in this solvent.

(19) Heitner, H. I.; Lippard, S. J. *Inorg. Chem.* **1974**, *13*, 815.

(20) (a) Lister, J. H. In *Advances in Heterocyclic Chemistry*; Katritzky, A. R., Boulton, A. J., Eds.; Academic Press: New York and London, 1966; Vol. 6, p 2. (b) Grimmet, M. R. In *Advances in Heterocyclic Chemistry*; Katritzky, A. R., Boulton, A. J., Eds.; Academic Press: New York and London, 1970; Vol. 12, p 103. (c) Breitmaier, E.; Voelter, W. In *Carbon C13 NMR Spectroscopy*; VCH: New York, 1990; p 281.

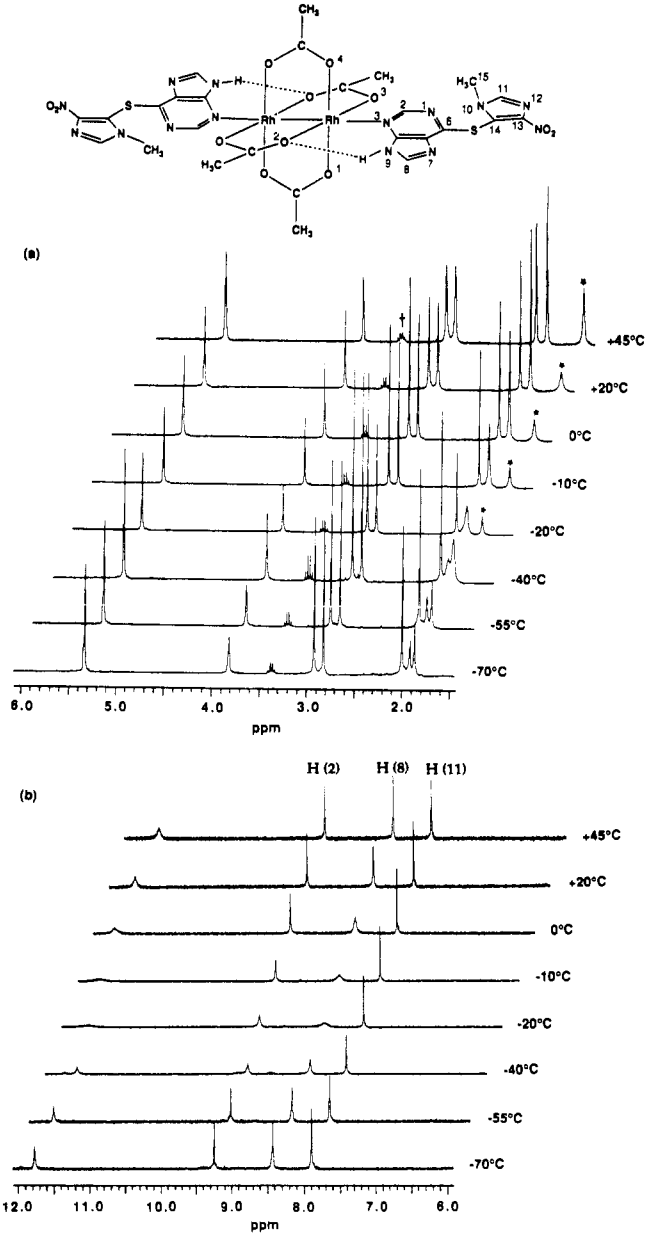

Figure 3. Variable temperature ^1H NMR spectra of $[Rh_2(OAc)_4(AZA)_2]\cdot 4DMAA$ (**1**) in CD_2Cl_2-d_2 from (a) δ +1.00 to +6.00 ppm and (b) from δ +6.00 to +12.00 ppm. The signal at ~5.3 ppm is due to the protic impurity in CD_2Cl_2-d_2. An asterisk denotes a signal due to solvent impurity which changes position and intensity with the temperature; this impurity proved not to be H_2O, because H_2O in CD_2Cl_2-d_2 resonates at ~5 ppm. A † indicates a signal due to residual Et_2O from washings.

rioazathioprine. In 50% and 100% deuteriated samples of 8-deuterioazathioprine, the integration area of the resonance due to H(8) diminishes to half of that of H(2) in the first case and disappears entirely in the second one respectively; this is in excellent agreement with previous observations of the reactions of purine derivatives with D_2O at elevated temperatures that are known to exchange the H(8) proton with deuterium.[2f,21] At room temperature in CD_2Cl_2-d_2, the ^1H NMR spectrum of **1** shows three aromatic protons for AZA at δ +9.28, +8.35, and +7.82 ppm, corresponding to H(2), H(8), and H(11), respectively (Figure 3b); the $CH_3(15)$ resonates at δ +3.85 ppm (Figure 3a). The large 0.67 ppm downfield shift of H(2) accords with the Rh-AZA binding through N(3), since it is well-known that upon metal coordination to ring nitrogens of purines, extensive π-electron redistribution of the ring occurs, rendering the protons adjacent to the binding site more acidic.[2f,20,22] The 0.22 ppm downfield shift of H(8) relative to free AZA is due to hydrogen bonding between N(9) and the carboxylate oxygens of the rhodium acetate. The downfield shift of H(11) as well as that of the $CH_3(15)$ of the imidazole ring are attributed to secondary electronic effects due to circulation of electron density within the rings. In Figure 3a, the three resonances at δ +2.97, +2.87, and +2.02 ppm are assigned to the dimethylacetamide which contains three magnetically nonequivalent methyl groups. The partial double bond character of the amide bond renders the two methyl groups bound to the nitrogen atom nonequivalent, thus giving rise to two discrete resonances for these groups at δ +2.97 and +2.87 ppm.

In order to further investigate the nature of the hydrogen bond between N(9) and O(1)/O(2), variable-temperature ^1H NMR data were carried out in CD_2Cl_2-d_2 over the temperature range +45 to −70 °C (Figure 3). At +20 °C, the acetate ligands exhibit only one resonance at δ +1.91 ppm which sharpens as the temperature is raised (Figure 3a). On the contrary, as the temperature is lowered below +20 °C, the resonance of δ +1.91 ppm broadens, eventually coalesces, and reappears as two separate signals in an intensity ratio of 1:1 between −20 and −40 °C. The low-temperature limiting values for the acetate resonances are δ +1.91 and δ +1.87 ppm, which integrate in a 1:1 ratio. Along with this salient feature of the spectrum, the resonance at δ +11.65 ppm (Figure 3b), assigned to the purine N(9)–H group of **1** (the resonance of the N(9)–H group can not be seen in the ^1H NMR spectrum of the free ligand due to its low solubility in CD_2Cl_2-d_2), broadens as the temperature is gradually lowered from +20 to 0 °C, and finally completely coalesces at −20 °C to reappear at ca. −40 °C. Concomitantly, the H(8) resonance at δ +8.35 ppm follows the behavior of the N(9)–H group, coalescing at −20 °C and becoming sharp again as the temperature is further lowered. These observations imply rapid rotation of the AZA ligand in the axial position of **1** at room temperature. This rapid rotation about the Rh(1)–N(3) bond renders all acetate groups magnetically equivalent for an intensity ratio of 4:2 between the CH_3COO and the $CH_3(15)$ groups of AZA. In contrast to this intramolecular rotation, which takes place at higher temperatures, this fluxional behavior is slowed as the temperature is lowered, thereby revealing the existence of an isomer containing two distinct acetate groups; this species may either be one in which the two AZA ligands are hydrogen bonded as in the solid state, that is to say with the AZA ligands essentially coplanar, or one in which the AZA ligands are hydrogen bonded to acetates at 90° with respect to each other. The ^1H NMR experiment does not permit the discrimination between two isomers of this type. No evidence was seen for a second isomer in the variable-temperature study, although its existence is predicated on the basis of the coalescence of the N(9)–H, H(2), and H(8) protons.

Electronic Spectroscopy. The red color of the adduct $Rh_2(OAc)_4(AZA)_2\cdot 4DMAA$ (**1**) is in agreement with an axial nitrogen donor ligand. With rhodium acetate compounds, colors range from red, pink, or violet for nitrogen donors, to blue or green for oxygen donors, and to orange for sulfur.[2b,c,f,23] The electronic spectrum of **1** in CH_2Cl_2 (Figure 4, Table V) consists of two bands each in the visible and the UV region. In going from the H_2O to the AZA adduct of $Rh_2(OAc)_4$, the higher energy visible absorption, band II (442 nm, sh), remains essentially constant in position, whereas band I (λ_{max} = 532 nm, ϵ_M = 368 M^{-1} cm^{-1}), experiences a blue shift. Indeed, band I is strongly influenced by changes in the axial ligand and shifts to higher energies in the following sequence according to the donor atom: $O < S < N_{sp^3} < N_{sp^2} \approx As < S = O$ (S bonded).[2f,23] In the UV region, band III (342 nm, sh) experiences a red shift as the axial

(21) Hadjiliadis, N.; Theophanides, T. *Inorg. Chim. Acta* **1976**, *16*, 67.

(22) (a) Hadjiliadis, N.; Theophanides, T. *Inorg. Chim. Acta* **1975**, *15*, 167 and references therein. (b) Hadjiliadis, N.; Theophanides, T. *Inorg. Chim. Acta* **1976**, *16*, 77–88 and references therein.

(23) Kitchens, J.; Bear, J. L. *J. Inorg. Nucl. Chem.* **1969**, *31*, 2415.

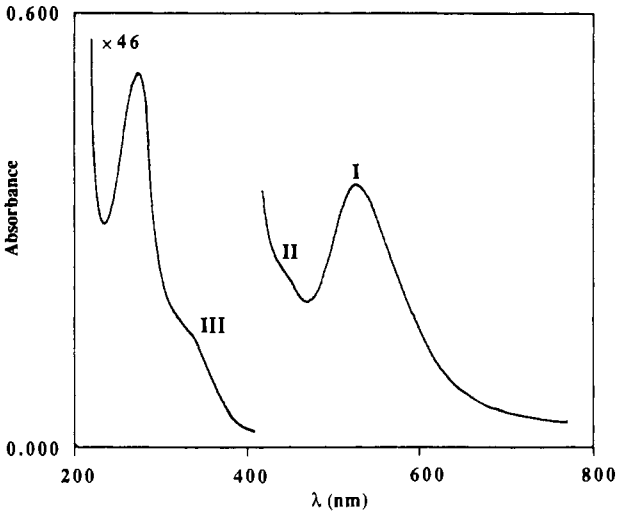

Figure 4. Electronic spectrum of $[Rh_2(OAc)_4(AZA)_2]\cdot 4DMAA$ (1) in CH_2Cl_2.

Table V. Electronic Spectral Data for $Rh_2(OAc)_4\cdot L_2$ Complexes[a]

	electronic spectral data		
compd	band I $\pi^*(Rh_2) \rightarrow \sigma^*(Rh_2)$	band II $\pi^*(Rh_2) \rightarrow \sigma^*(Rh\text{-}O)$	band III $\sigma(Rh_2) \rightarrow \sigma^*(Rh_2)$
$Rh_2(OAc)_4(H_2O)_2$[b]	584[e]	442 sh	250 sh
$Rh_2(OAc)_4(DMAA)_2$[c]	606	453 sh	354 sh
$Rh_2(OAc)_4(AZA)_2$[d] (1)	532	442 sh	342 sh

[a] Assignments for the transitions are taken from ref 15b. [b] Values from refs 15b, 23 for a sample of $Rh_2(OAc)_4(H_2O)_2$ prepared in H_2O. [c] For a sample of $Rh_2(OAc)_4(H_2O)_2$ prepared in DMAA. [d] For a sample of 1 prepared in CH_2Cl_2. [e] λ_{max} values are given in nm.

ligand is changed from H_2O to AZA. Unfortunately, band IV for 1, which is in the region below 230 nm, could not be observed due to limitation of the solvent (CH_2Cl_2) which begins to cut off in the UV region at 252 nm. The absorption at λ_{max} = 279 nm ($\epsilon_M = 2.4 \times 10^4\ M^{-1}\ cm^{-1}$) is ligand based.[24]

Cyclic Voltammetry. The electrochemical properties of 1 as determined by cyclic voltammetry are characterized by a one electron reversible oxidation at $E_{1/2}$ = +1.14 V vs Ag/AgCl, at 200 mV/s, in CH_2Cl_2 containing 0.1 M $(TBA)BF_4$ as the supporting electrolyte. The $i_{p,a}/i_{p,c}$ ratio is ~1, the $E_{p,c} - E_{p,a}$ separation is 70 mV and plots of $i_p/v^{1/2}$ were approximately constant over sweep rates of 50–500 mV s^{-1}. The Cp_2Fe/Cp_2Fe^+ couple exhibits a separation of 70 mV under the same experimental conditions. This behavior is quite typical for $Rh_2(OAc)_4L_2$ complexes, all of which exhibit a one electron oxidation process at potentials near +1.0 V.[15]

Factors Affecting Tetrakis(μ-acetato)dirhodium Binding to Azathioprine. The most interesting structural feature of 1 is the fact that the metal binds to the pyrimidine N(3) of AZA, unlike the few known purines which bind to dirhodium tetraacetate through the imidazole ring N(7) or N(9) sites.[2f,h,i,k,m,25] Presumably, steric constraint imposed by the octahedral environment about the rhodium atom[26b] together with the bulk of the imidazole ring on S(1) inhibits N(7) binding (there is a case of a Rh(I) carbonyl monomer that binds to the N(3) atom of 8-aza-9-benzyladenine).[27] In DNA it is highly probable that the N(3) of the purine skeleton is subjected to steric hindrance in both pairs (A-T and G-C) to a much greater extent than N(7) due to the relative proximity of the phosphate groups and due to the more central position of N(3) on the helix of the nucleic acid, whereas N(7) is located more peripherally.[27,28] It is, therefore, unlikely that the N(3) of a DNA purine would bind to a dimetal tetracarboxylate cage such as was seen in this study. It is very likely that, for these steric reasons, rhodium carboxylates do not react with polycytidylic acid, in which N(3), the preferable binding site for other metals, is flanked by the bulky carbonyl O(2) and amino N(4) groups of cytidine.[25,26a,c] Steric arguments are also reasonable for explaining why the rhodium atom in 1 does not attach to the thioether atom S(1), although in other cases of thioethers it does.[15a,3c,29] The N(12) of the imidazole ring is not preferred, presumably due to the presence of the electron withdrawing NO_2 group,[30a] although binding of rhodium acetate to 5-nitroimidazole has been observed.[30] Apart from the axial interaction of N(3), in 1, N(9)–H forms a hydrogen bond with the acetate O(2); this resembles the hydrogen bond formed between dirhodium carboxylate oxygens and the exocyclic N(6) group of N(7)-bound 1-methyladenosine (N6–H–O1(OAc) = 2.97 (2) Å)[2m] and polyadenylic bases.[2h,i,26a] The formation of this intramolecular hydrogen bond between the base substituent and the acetate oxygens is claimed to favor axial coordination of adenosine to rhodium acetate as opposed to guanosine;[2h,26c] electrostatic repulsion between O(6) of guanine and the acetate oxygens may be responsible for the lack of reactivity between polyguanylic acid and dirhodium tetraacetate.[26a,c]

Conclusion. The structure of the bis adduct of $Rh_2(OAc)_4$ and AZA has been determined and found to exhibit some interesting structural features that bear on the general observations of $Rh_2(OAc)_4$ reactivity with purines. In this case, N(3) is favored because of its high basicity[28] as well as for steric reasons. The elucidation of the different interactions in this unusual structure and its similarities to the known rhodium tetraacetate complexes of nucleotides imply that for an octahedral complex to have antitumor activity, not only does the electronegativity of the various binding sites of the ligand play a major role but stereospecific interligand interactions are important as well. These structural studies, aimed at unraveling the selective binding properties of dinuclear rhodium complexes, are useful tools for understanding the mechanism of action of such chemotherapeutic agents. Future work on the antimetabolite azathioprine will focus on efforts to crystallize complexes of this drug with other tetracarboxylates such as $Rh_2(O_2CCF_3)_4$, as well as with other platinum group metals in order to make comparative studies correlating its various binding sites with the "softness" or "hardness" of the metal. From a biological point of view, preliminary studies of the anticancer activity of 1 on different tumor cell lines, namely L1210 and Sarcoma 180 show positive antitumor activity and need to be further investigated. For other rhodium carboxylate complexes with biologically active drugs, the complex has been found to have a chemotherapeutic index superior to that of the free carboxylate.[21]

Acknowledgment. We thank Professor G. Pneumatikakis of the University of Athens for helpful discussions and a reviewer for helpful suggestions. We are grateful to the National Science

(24) Wilson, W. P.; Benezra, S. A. In *Analytical Profiles of Drug Substances*; Florey, K., Ed.; Academic Press: New York, 1981; Vol. 10, p 29.
(25) Aoki, K.; Yamazaki, H. *J. Chem. Soc., Chem. Commun.* **1980**, 186.
(26) (a) Aoki, K.; Yamazaki, H. *J. Chem. Soc.* **1984**, *106*, 3691. (b) Aoki, K.; Yamazaki, H. *J. Chem. Soc.* **1985**, *107*, 6242. (c) Aoki, K.; Hoshino, M.; Okada, T.; Yamazaki, H.; Sekizawa, H. *J. Chem. Soc., Chem. Commun.* **1986**, 314 and references therein.
(27) Sheldrick, W. S.; Günther, B. *Inorg. Chim. Acta* **1988**, *152*, 223.
(28) Pullman, B.; Pullman, A. In *Quantum Biochemistry*; Interscience: New York, 1963; pp 230, 235.
(29) (a) Clark, R. J. H.; Hempleman, A. J.; Dawes, H. M.; Hursthouse, M. B.; Flint, C. D. *J. Chem. Soc., Dalton Trans.* **1985**, 1775 and references therein. (b) Faraglia, G.; Graziani, R.; Volponi, L.; Casellato, U. *Inorg. Chim. Acta* **1988**, *148*, 159.
(30) (a) Bales, J. R.; Mazid, M. A.; Sadler, P. J.; Aggarwal, A.; Kuroda, R.; Neidle, S.; Gilmour, D. W.; Peart, B. J.; Ramsden, C. A. *J. Chem. Soc., Dalton Trans.* **1985**, 795. (b) Goodgame, D. M. L.; Lawrence, A. S.; Slawin, A. M. Z.; Williams, D. J. *Inorg. Chim. Acta* **1986**, *125*, 143. (c) Dyson, T. M.; Morrison, E. C.; Tocher, D. A.; Dale, L. D.; Edwards, D. I. *Inorg. Chim. Acta* **1990**, *169*, 127.

Foundation for X-ray equipment grants (CHE-8403823 and CHE-8908088) and NMR equipment (CHE-88-00770) and a PI grant to K.R.D. (CHE-8919915). Mass spectral data were obtained at the Michigan State University Mass Spectrometry Facility which is supported, in part, by a grant (DRR-00480) from the Biotechnology Research Technology Program, National Center for Research Resources, National Institutes of Health. Grateful acknowledgement is also made to the Wellcome Co. for a loan of azathioprine.

Supplementary Material Available: Tables of crystallographic parameters, atomic positional parameters and equivalent isotropic displacement parameters, full bond distances and angles, and anisotropic thermal parameters (9 pages). Ordering information is given on any current masterhead page.